

Normalized increment of crystal mass as a possible universal parameter for dendritic growth

L. M. Martyshev* and P. S. Terentiev

Ural Federal University, 19 Mira Street, Ekaterinburg 620002, Russia and Institute of Industrial Ecology, Russian Academy of Sciences, 20 S. Kovalevskaya Street, 620219 Ekaterinburg, Russia

(Received 16 January 2012; published 27 April 2012)

The unsteady growth of ammonium chloride dendrites during crystallization from an aqueous solution in a thin capillary is experimentally investigated. The dependence of the crystal area S on the time t for various sectors located along primary branches and side branches is measured. The hypothesis that the ratio between the area change and the area itself [$S'(t)/S(t)$] is one and the same for different but simultaneously growing parts of an unsteady dendrite is advanced and confirmed. This conclusion allows a curve to be proposed to describe the evolution of the dendrite area (or its part), with the form $S(t) = \text{const } t^a \exp(-bt)$, where a and b are the parameters whose values are determined in the paper. The nondimensionalization of $S(t)$ and $S'(t)/S(t)$ (using the full dendrite growth time) produces simple one-parameter functions that depend on a single parameter a (which is presumably associated only with the physical and chemical characteristics of the crystallized system and, in our case, is equal to 1.7 ± 0.2).

DOI: [10.1103/PhysRevE.85.041604](https://doi.org/10.1103/PhysRevE.85.041604)

PACS number(s): 68.70.+w, 81.10.Aj

I. INTRODUCTION

Interest in the investigation of dendrite growth during crystallization arose long ago¹ and has persisted until the present [2–9]. This interest is primarily connected with the fact that these structures often form during the solidification of melts and determine many properties of metal ingots [2–4]. In addition to researchers in material science, profound interest in dendrite growth has been shown by researchers studying various problems in the physics of nonequilibrium processes [5–9]. This breadth of interest occurs because the dendrites form in multiple so-called nonequilibrium (or dissipative) processes, which are commonly observed in nature. There are many examples of the formation of dendritelike structures, such as lightning discharges, growing trees, and the development of transport infrastructure [9,10]. Nature often chooses these structures when it is necessary to dissipate or remove a nonequilibrium state (during supercooling, supersaturation, changes of electric potential, etc.) that occurs for some reason. Consequently, researchers study dendrite crystallization as an example that may provide insight into the general regularities of nonequilibrium processes. The example is remarkable because it permits easy experimental investigation, the underlying physical processes are well studied, and the describing equations are relatively few and simple [5–7].

Many papers have dealt with the regularities of dendrite development during crystallization (see, for example, reviews [5–8]). The relation between the external shape (or the morphology) and the growth rate (or the kinetics) of the dendrite is an extensively studied field. At present, a dendrite is considered to have a rigorously defined (close to parabolic) shape and a precise growth rate at a certain supercooling or supersaturation. When the supercooling or supersaturation increases, the dendrite growth rate (V) increases, and the dendrite becomes sharper (the dendrite tip radius R decreases).

It has also been shown that the quantity VR^2 in the first approximation does not depend on the supercooling or supersaturation, but it is determined by the material parameters of the crystallized system. These results have received both experimental and theoretical confirmation (see, for example, [5–8]), and they represent important achievements; however, many questions remain open. First, these facts relate to steady dendrite growth. However, it is difficult to precisely detect this dendrite growth stage (especially for dendrites that grow under natural uncontrolled conditions rather than laboratory and controlled conditions, in which supersaturation or supercooling is artificially maintained). Indeed, a dendrite crystal has three growth stages: origination, approximately steady growth, and rate decrease and stoppage (when supercooling or supersaturation is removed as a result of crystallization). Obviously, the constancy of VR^2 does not hold during the entire interval of dendrite growth.² Second, the obtained results are not applicable to side branches. Indeed, the sidebranches grow at slightly lower supercooling/supersaturation, and they exhibit a smaller growth rate than that of the primary branch. According to the VR^2 constancy criterion, side branches should have blunter tips. However, in actual practice, their tips usually have a considerably smaller radius of curvature than that of the primary branch. Consequently, researchers aiming to confirm or verify the constancy of VR^2 are forced to artificially divide the dendrite into the primary branch (which is grown in conformity with the theory) and the side branches (which do not conform to the theory). This artificial division leads to some loss of universality and practical significance of the results.³

²When decreasing supercooling/supersaturation, R increases tending to some constant value and the rate is reduced to zero. It should be noted that a number of recent experiments (see papers [8], [11–13]) called into question the independency of VR^2 from supersaturation even in the case of steady growth.

³Indeed, when we focus the microscope on an arbitrary location in the solution and find a dendrite, we cannot predict what we will see. It

*leonidmartyushev@gmail.com

¹Thus, as far back as 1611, Kepler dedicated his paper to an ice dendrite, i.e., a snowflake [1].

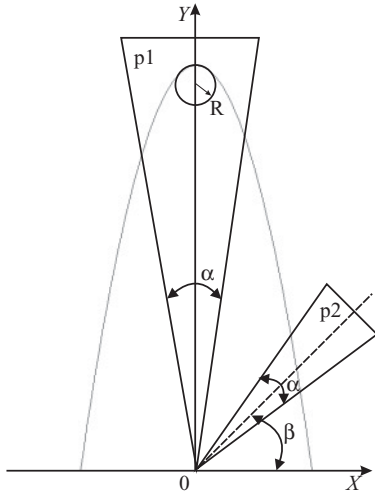


FIG. 1. Parabola with different sectors, for which the area is calculated.

Let us make an intermediate summary. Dendrite crystallization is a common phenomenon in nature. The parameter VR^2 cannot assume a universal role because it is not applicable to arbitrary (unsteady) dendrite time evolution intervals, and it fails to describe the morphokinetics of the dendrite side branches (it is only applicable to the region near the tip of the primary branch). If such a universal parameter exists, it remains unknown; however, we can provide some reasoning to indicate that such a parameter evidently exists.

A dendrite represents a certain ordered set of branches with parabolalike shapes (for simplicity and definiteness, we shall consider the two-dimensional case and crystallization from a solution). Let us consider a single parabola and select a certain sector therein with an arbitrary angle α (for example, p1 in Fig. 1). The equation of the parabola moving along the OY axis direction at a rate given by $V(t)$ and with a tip radius described by $R(t)$ has the following form:

$$y(x, t) = -x^2 / [2R(t)] + \int_0^t V(t) dt. \tag{1}$$

As a result, the parabola area S can be written as follows:

$$S(t) = 2 \int_0^{d(t)} y(x, t) dx - y(d(t), t) d(t), \tag{2}$$

where t is the time and $d(t)$ is the positive solution of the equation $x \operatorname{ctg}(\alpha/2) = -x^2 / [2R(t)] + \int_0^t V(t) dt$.

It is shown that the specific change of the crystal area (which can also be identified as the increment per unit of crystal area, the normalized area increment, or the relative increment)

may be a primary branch with secondary branches, or it may be a large and detached (as a result of the increase of the side-branch intervals because of period doubling) secondary branch with forming tertiary branches. In the second case, the researcher can take the secondary branch as a primary branch, even when a different spatial scale is used (when zooming in with the microscope).

$S'(t)/S(t)$ has an interesting property.⁴ Let us calculate this quantity for the two simplest and most widespread crystallization models.

(i) We shall assume that $V(t)$ and $R(t)$ are arbitrary constants (related to supersaturation, diffusivity, etc., but independent of time); i.e., steady dendrite growth occurs. In this case, for small angles α , as follows from (1) and (2), $S'(t)/S(t) = 2/t$. Thus, this quantity proves to be independent of both the supersaturation and other crystal characteristics.

(ii) We shall assume that the parabolic crystal grows under quasisteady diffusion-limited conditions. In this case, it is known that $V(t) = \Omega/\sqrt{t}$ and $R(t) = \Xi\sqrt{t}$, where Ω, Ξ are some constants related to supersaturation and the physical and chemical parameters of the considered crystallized system [18,19]. In this case, (1) and (2) can be used to show that $S'(t)/S(t) = 1/t$. Moreover, unlike the previous case, this ratio proves to be true for any angle α .

Thus, the simplest models considered indicate the interesting behavior of the quantity $S'(t)/S(t)$. This quantity has a power-law dependence on time only, during which the parabolic⁵ dendrite grows in the sector selected along its direction of growth. If the selected sector is at some angle β to the direction of growth (Fig. 1), the quantity $S'(t)/S(t)$ becomes dependent on many quantities, and there is no such simple and universal power-law dependence on time. According to the analysis results, the numerical factor that multiplies time (in the considered cases, it is 0.5 or 1) depends not only on the dependence of V and R on time but also on the shape of the sector in which the dendrite is observed (in particular, the numerical factors turn out to be twice smaller for rectangular sectors). Additionally, it can be easily verified that the numerical factor depends on the spatial dimension of the problem.

A real dendrite consists of a primary branch and side branches with parabolalike shapes. Will the experiment confirm the constancy of the quantity $S'(t)/S(t)$ for various dendrite branches growing simultaneously? Will this quantity depend on the angles α and β of the sectors? How close, in the case of real unsteady dendrites, will the quantity $S'(t)/S(t)$ be to the dependence that is given above for the simplest models of steady and quasisteady growth? The search for the answers to these questions forms the objective of the present study.

II. EXPERIMENTAL PROCEDURE

A. Experimental setup

An aqueous solution of ammonium chloride (NH_4Cl) was selected as a dendrite growth system (its crystallization has been the subject of numerous studies [20–28]).

An NH_4Cl solution with a concentration of 43.6 g/100 g H_2O was prepared, corresponding to a saturation temperature of 35°C, and the solution was placed between two

⁴This parameter (which is directly proportional to entropy production density) has attracted interest because of papers [14–17].

⁵The parabolicity of the dendrite front is not of fundamental importance, and it can be easily proved that similar conclusions will also be true; for example, in the case of rounded or rectilinear shapes of the crystallization front.

18 × 18 × 0.2 mm glass plates. The solution thickness between the panes did not exceed 0.05 mm. Because the diffusion length was not less than $2D/v \approx 0.5$ mm (where v and D are the growth rate and the dendrite diffusivity, respectively, and $D = 2.6 \times 10^{-5}$ cm²/s [24]), the cell prepared in such a manner can be considered a quasi-two-dimensional cell. The prepared cell was held at a temperature exceeding the saturation temperature by 5°C to homogenize the solution in the cell and remove any possible crystal nuclei. The waiting time was not less than 10 min. Then, the cell was placed on the heavy objective table of a BIOLAR PI microscope at a temperature of 20°C. Because of the thin cover glasses and the small thickness of the solution between them, the cell attained a temperature of 20°C within 2–3 s. Video recording of the freely growing dendrites was started after 10–15 s. Only single freely growing dendrites that were separated from the neighboring dendrites and the borders of the crystallization cell by at least the diffusion length were targeted for observation and recording (usually at 110-fold magnification). In the vast majority of cases (94%), dendrite growth was observed in which the secondary branches were oriented in the $\langle 100 \rangle$ direction.⁶ No tertiary branches were observed. In total, 96 samples were studied. The dendrites under study were oriented almost parallel to the glass plates. During the experiments, both less (Fig. 2) and more (Fig. 3) symmetrical dendrites were observed. The number of less symmetrical dendrites was slightly greater (approximately 65% of those observed). Recording was carried out using a digital video camera with a resolution of 720 × 576, and the size of a pixel at the selected zoom was 0.00068 mm.

B. Image processing and measurement errors

The projection area of the dendrite onto the cell surface⁷ was measured as follows:

(1) A video clip of the dendrite growth was divided into separate frames with a minimum frequency of 1 frame/s. These frames were converted to gray scale. Then, each frame was individually processed. For this purpose, a special software tool was written in the MATLAB (image processing toolbox) environment.

(2) The detection of the crystal contour in each frame was the most complicated stage of image processing. This complexity arose from the automation needed for the processing because the number of frames for each video clip could amount to approximately 1000. Two standard methods were used: the method of morphological erosion and the method of brightness histogram adjustment [29]. The first method is based on the detection of boundaries from the brightness gradient

⁶So-called irregular patterns [22] were observed in 4% of the cases. A separate paper will be dedicated to the discussion of the kinetics of these crystals.

⁷This value is directly proportional to the crystal mass. Indeed, the observed dendrites are three-dimensional (e.g., they are a paraboloid near a tip), however, side branches do not grow perpendicularly to the glasses due to the cell's geometry (Figs. 2 and 3). As a conclusion, the projection area of the dendrite onto the cell's surface is a close approximation of the volume or mass (if the crystal density is constant) of the whole crystal.

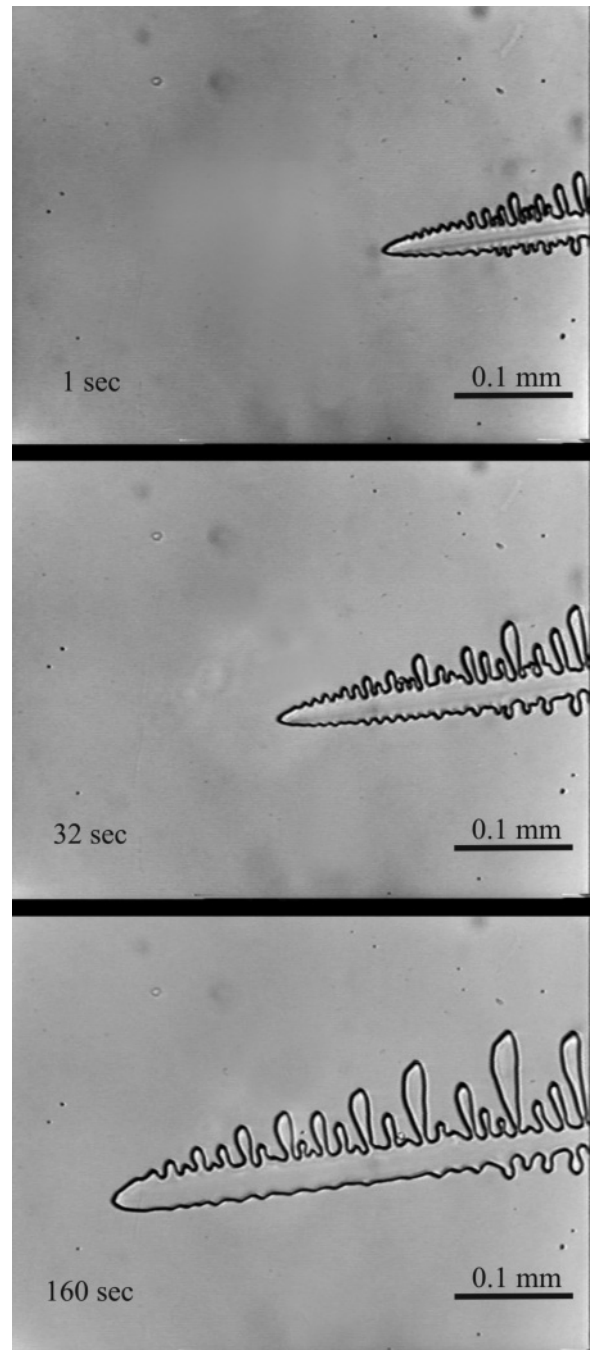


FIG. 2. Frames of an asymmetric dendrite of ammonium chloride growing from the aqueous solution.

difference. This produces multiple unconnected fragments of the crystal perimeter located along its apparent boundary. The fragments form a continuous line by thickening. This procedure leads to a slightly overestimated value of the crystal area because of boundary thickening. The second method presupposes the histogram adjustment (brightness redistribution). The crystal object in the picture usually has a specific brightness interval that does not cover the entire possible range (from 0 to 255). The image pixels whose brightness values fall outside the interval are assigned the values of the brightness interval boundary. This manipulation

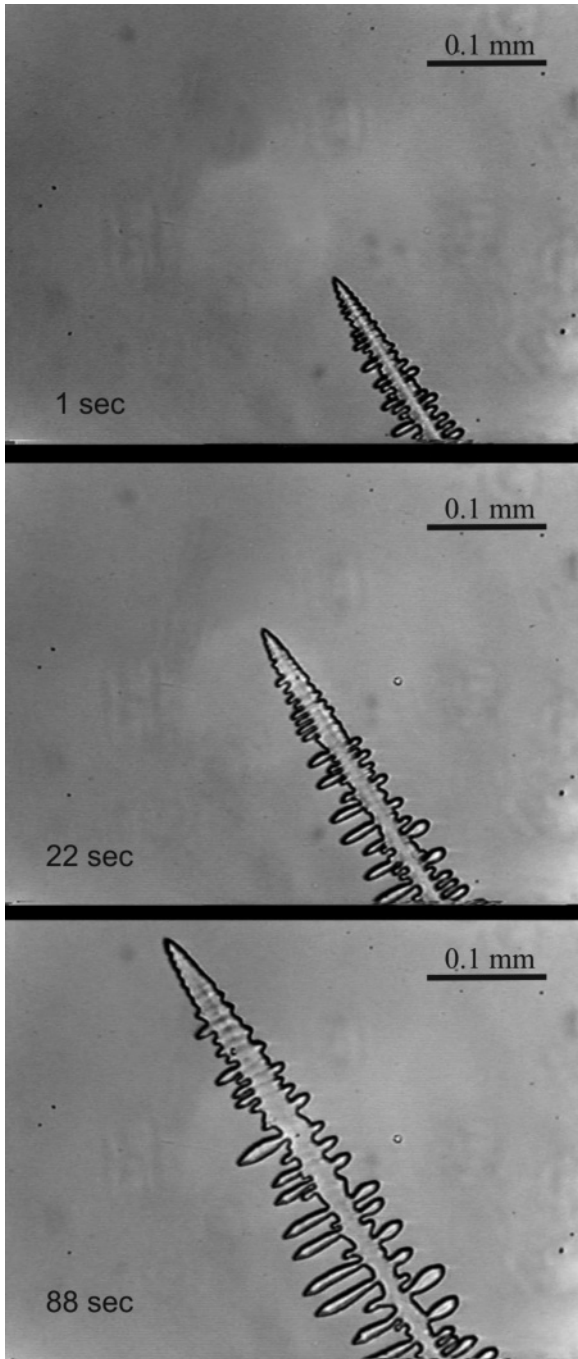


FIG. 3. Frames of a symmetric dendrite of ammonium chloride growing from the aqueous solution.

provides noise reduction and improves the crystal-background contrast. This improvement enables segmentation (detection) of the edge pixels with threshold filtering. Neither the first nor the second method has full process automation. For example, it is necessary to set the minimum brightness gradient difference that is to be considered in the first method, and the brightness interval and threshold value must be set in the case of the second method. However, if these parameters are set for several frames at different moments of dendrite growth, then all intermediary frames can be processed automatically. Testing



FIG. 4. Example of the crystal contour detection and the image binarization for the structure shown in Fig. 2 (160 s).

of these two methods on frames containing structures with known areas and video quality similar to that of the experiment has shown that the method based on histogram adjustment has greater accuracy and stability in the case of automatic area calculation. This method was selected as the main method for image processing.

(3) After detecting the dendrite contour, the images were binarized. The region belonging to the crystal was assigned one color (black), and the solution was assigned another color (white) (Fig. 4). The crystal area was found by simply counting the black pixels. The pixels were converted to mm using the templates of known size that were recorded under the same conditions.

(4) As mentioned above, the detection of the crystal boundary inevitably introduces error in the crystal area calculation. Obviously, a greater ratio of the characteristic size of the crystal R to the size of the pixel d produces smaller error. The relative error of the area calculation with the size determination accuracy of one pixel can be obtained from $\delta_R = 2d/R$. Consequently, for a crystal size of 10 pixels (and a corresponding area of approximately 100–300 pixels), the absolute error of the area determination is 20%, and it is only 2% for a characteristic size of 100 pixels. This estimate shows that an area measurement with an accuracy of approximately 10% is only possible for the crystal sections with areas of approximately 10^3 pixels. In the considered case of the determination accuracy of one pixel, the relative determination error of the crystal area increment per unit time is approximately $\delta_\Delta = 2d/\Delta$, where Δ is the change of the crystal size (it is assumed that the growing crystals are quite large, and one can neglect the error of area determination). The determination error of $[S'(t)/S(t)]$ is $\sqrt{\delta_\Delta^2 + \delta_R^2}$. For a crystal with a characteristic dimension of 100 pixels and an increment of 10 pixels per unit time, it is easy to determine that the error will be at least 20% (however, the area change will be only 1%). Thus, based on the above, there is a restriction for both the sector size during measurement of the crystal area (it should not be very small) and for the observation time (such that the area change is not excessively small). Therefore, in the case of the so-called sigmoid curves (see below), the dependence of the crystal area (mass) on time and the normalized area increment can be determined with adequate accuracy only in the middle section. Indeed, the crystal size is small (and δ_R is high) at the initial stage, and the area change is very small (and the role of δ_Δ increases significantly) at the final stage. The above issue will be considered in the next section, when the results of the direct and indirect measurements are presented. The values will be given in the time interval for which their errors do not exceed 20%.

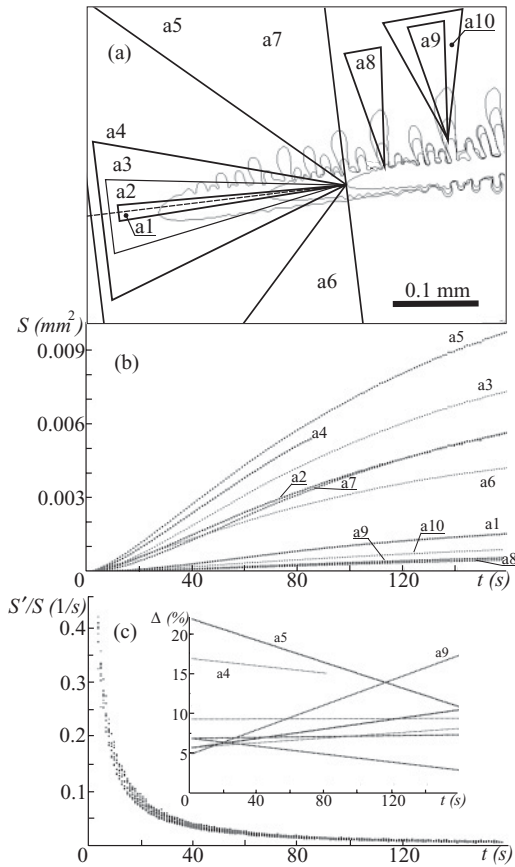


FIG. 5. Measurement results of the dendrite shown in Fig. 2. (a) Sectors used for area measurement. Sector sizes (in radians) are as follows: $a_1 = 0.02\pi$, $a_2 = a_8 = a_9 = 0.1\pi$, $a_3 = a_{10} = 0.2\pi$, $a_4 = a_6 = a_7 = 0.5\pi$, and $a_5 = \pi$. The sector a_5 contains the whole dendrite grown for the selected moment of time, and sectors a_6 and a_7 contain only the lower and the upper parts of the dendrite, respectively. (b) Values of the area S relative to the dendrite growth time t for different sectors. (c) Values of the normalized area increment $S'(t)/S(t)$ relative to the dendrite growth time t for different sectors. The inset shows the relative difference between $S'(t)/S(t)$ of each sector and $S'(t)/S(t)$ for the sector a_2 .

III. RESULTS AND DISCUSSIONS

In accordance with the goal of this study, the mass increment (equivalent to the area increment in the quasi-two-dimensional case considered here) was observed in sectors of different sizes oriented along various dendrite branches [see Figs. 5(a) and 6(a)]. The areas and increments were measured and compared in every sector at the same time. Correspondingly, the vertices of these sectors were placed on the crystal surface at some selected moment of time, and the crystal area contained in the selected sector was measured. The results were processed for different time intervals of the dendrite growth (limited to its beginning and end). The measurement results of the area $S(t)$, the ratio $S'(t)/S(t)$, and the deviations of $S'(t)/S(t)$ for various dendrite sectors are given in Figs. 5(b) and 5(c) and 6(b) and 6(c).⁸

⁸Here and below, the results of two typical experiments out of the whole array of the obtained experimental data are presented.

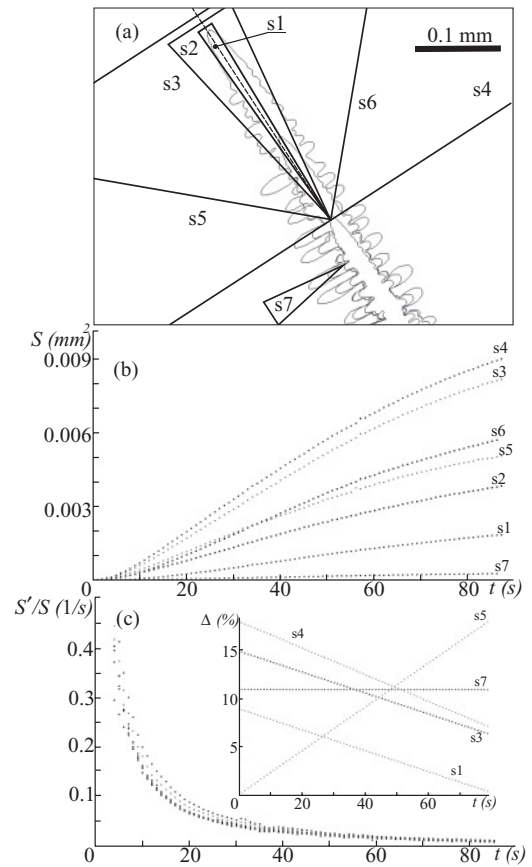


FIG. 6. Measurement results of the dendrite shown in Fig. 3. (a) Sectors used for area measurement. Sector sizes (in radians) are as follows: $s_1 = 0.02\pi$, $s_2 = s_7 = 0.1\pi$, $s_3 = s_5 = s_6 = 0.5\pi$, and $s_4 = \pi$. The sector s_4 contains the whole dendrite grown for the selected moment of time, and the sectors s_5 and s_6 contain only the left and the right part of the dendrite, respectively. (b) Values of the area S relative to the dendrite growth time t for different sectors. (c) Values of the normalized area increment $S'(t)/S(t)$ relative to the dendrite growth time t for different sectors. The inset shows the relative difference between $S'(t)/S(t)$ of each sector and $S'(t)/S(t)$ for the sector s_2 .

The following conclusions can be drawn from the presented results:

(1) The dependence of the area on the time belongs to a sigmoid-type (S-shaped) curve. For different observation sectors, a significant difference is observed in the values of both $S(t)$ (sometimes by factors of 10) and the crystal area increment $S'(t)$ (as an example, see Fig. 7).

(2) In spite of the significant difference between $S(t)$ and $S'(t)$ for different sectors, the values of $S'(t)/S(t)$ agree in the vast majority of cases within a range of 15% (i.e., within the limits of the experimental error). This value exhibits a hyperbolic dependence on time. The agreement is observed for the small angles of 0.02π and 0.1π , but it is also observed for large angles of 0.5π and π , which cover the whole dendrite and all side branches. The results given in Figs. 5(c) and 6(c) show that the dependences of $S'(t)/S(t)$ for the side branches (sectors a_8 – a_{10} , s_7) and the primary branches (sectors a_1 and a_2 , s_1 and s_2) are the same, within the limits of the experimental error. Let us specifically note the agreement

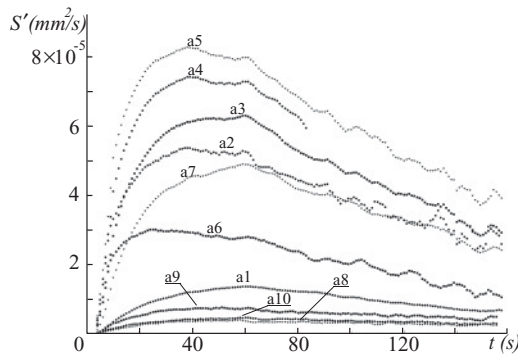


FIG. 7. Dependence of the area increment $S'(t)$ on the dendrite growth time t for different sectors of the structure shown in Fig. 5.

within the error limits of the normalized increment for the dendrite parts growing in sectors a7 and a6. These identical sectors divide the dendrite into two parts with unequal areas. Because the first sector (a7) contains the upper half of the dendrite with the developed side branches, and the second sector contains the lower half of the dendrite with almost no branches, the agreement of the normalized mass increment is an uncommon result.

Thus, the presented measurement results confirm the hypothesis of the universality of the normalized crystal mass increment $S'(t)/S(t)$ stated in the Introduction (i.e., the found parameter is the same for different simultaneously growing branches of the unsteady dendrite). However, two critical questions arise:

(i) Is it possible that other quantities composed of $S'(t)$ and $S(t)$ may also be nearly equal for different sectors within the limits of the experimental error, so that no positive conclusion can be drawn from the above results?⁹ Figure 8 shows an example of two calculations of the quantities $S'(t)/S^2(t)$ and $S'(t)/L(t)$ [where $L(t)$ is the length of the crystal boundary inside the sector] for sectors a2 and a5. These derived quantities differ by 80%–350% for the two sectors, which enables this uncertainty to be resolved.

(ii) What will happen if the sector in which the dendrite area is measured is directed at an angle to the growing dendrite branch? Will differences occur here, by analogy with the simplest case considered in the Introduction (e.g., sector p2, Fig. 1)? The measurements have indicated that the answer is affirmative. As Fig. 9 shows, the differences between the values of $S'(t)/S(t)$ increase sharply for different turns of the sector. The error is 30%–70% when for a turn of 30°, and it is >120% for a turn of approximately 45°.

Let us refer to a more detailed analysis of the dependence of $S'(t)/S(t)$. Table I gives factors of the experimental point approximation using the following three-parameter dependence: $a/t^c - b$. The correlation coefficient is at least 0.99. According to the table data, $c = 0.97 \pm 0.06$ for the dendrite

⁹The more so because, due to the sigmoid-type curves of $S(t)$, the numerator of the ratio $S'(t)/S(t)$ decreases and the denominator increases, and, as a consequence, the value under study becomes very small with time and its difference for different sectors is hard to determine.

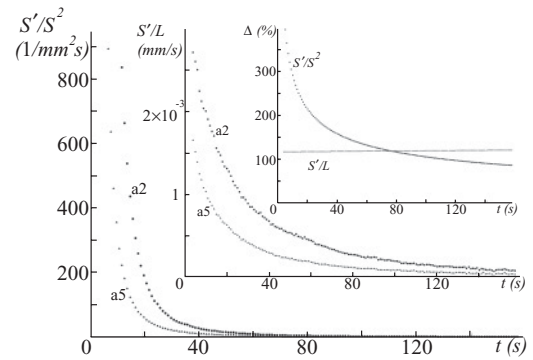


FIG. 8. For the sectors a2 and a5 (Fig. 5), the dependence of the dendrite area increment divided by the squared area [$S'(t)/S^2(t)$] and the dependence of the dendrite area increment divided by the perimeter of the crystal boundary inside the sector [$S'(t)/L(t)$] are given. The inset shows the relative deviation of the values of $S'(t)/S^2(t)$ measured for the sectors a2 and a5 and the relative deviation of the values of $S'(t)/L(t)$ for the same sectors.

shown in Fig. 2, and $c = 1.00 \pm 0.04$ for the dendrite in Fig. 3 (with a significance level of 95%). Thus, the factor multiplying the time can be assumed to be equal to one within the accuracy of observation. Consequently, the use of the two-point approximation $a/t - b$ is possible.

Table II gives factors of the experimental point approximation using the two-parameter dependence given by $a/t - b$. The correlation coefficient remains at least 0.99. The factors for different sectors of the same dendrite are close to each other, and their distribution is nearly normal. Furthermore, in terms

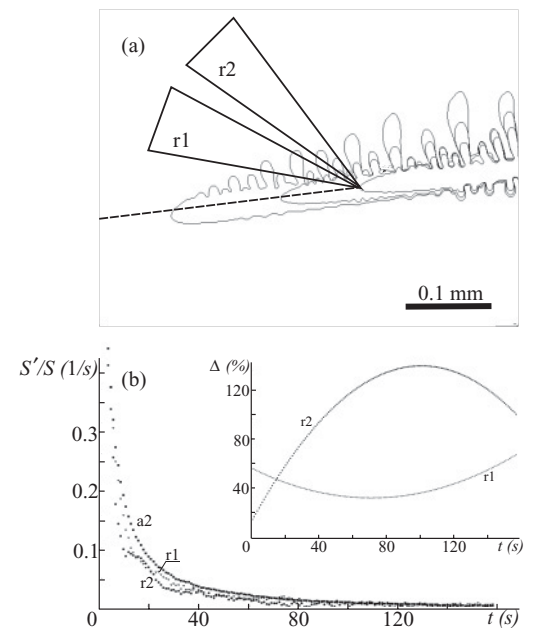


FIG. 9. (a) Sectors used for area measurement: r1, r2 with turns of 30° and 45° with respect to the primary dendrite branch. Sector sizes (in radians) are as follows: $r1 = r2 = 0.1\pi$. (b) Values of the normalized area increment $S'(t)/S(t)$ relative to the dendrite growth time t for the sectors. The inset shows the relative difference between $S'(t)/S(t)$ of each sector (r1 or r2) and $S'(t)/S(t)$ for the sector a2 [Fig. 5(a)].

TABLE I. Values of the three-parameter approximation $a/t^c - b$ of $S'(t)/S(t)$ for different sectors.

Factors \ Sectors	Sectors																
	a1	a2	a3	a4	a5	a6	a7	a8	a9	a10	s1	s2	s3	s4	s5	s6	s7
a	1.49	1.92	1.65	1.72	1.71	1.89	1.56	1.55	1.43	1.07	1.99	1.77	1.66	1.92	1.72	1.87	1.51
b	0.02	0.01	0.01	0.01	0.01	0.00	0.01	0.01	0.01	0.02	0.02	0.02	0.01	0.01	0.01	0.01	0.02
c	0.89	1.00	0.98	1.02	1.05	1.09	1.01	0.95	0.89	0.81	0.96	0.97	0.99	1.06	1.01	1.07	0.95

of the experimental accuracy, the values of the factor a agree for sectors of *different* dendrites within the error limits, and the values of the factor b do not agree. Therefore, it is reasonable to consider one average value of the factor a , 1.7 ± 0.2 . For the factor b , the average values do not vary for different sectors of one dendrite, but they do vary for different dendrites. Thus, $b = 0.007 \pm 0.002$ for the dendrite shown in Fig. 2, and $b = 0.014 \pm 0.002$ for the dendrite in Fig. 3. The use of a one-parameter approximation of the form a/t proves to be too crude for the available experimental data.

If we know that $S'(t)/S(t) = a/t - b$, the analytical dependence for $S(t)$ can be found. The differential equation is solved as follows: $S(t) = Ct^a \exp(-bt)$, where C is a constant that can be found using the known value of the crystal area at some moment of time.

The obtained factor a proves to be similar to the values obtained analytically when the “growth” is considered to be parabolic (see the Introduction). The factor is equal to 2 if the steady growth (kinetically limited) regime is assumed, and it equals 1 for the quasisteady growth (diffusion-limited) regime. The obtained value lies between these limits. The factor b characterizes the decrease of the crystal growth rate.¹⁰ However, this rate decrease is not connected with the geometric features of the growing crystal (as it is in the case of diffusion-limited growth in a solution with a constant supersaturation control), but it is most likely related to the ratio between the initial supersaturation and the time at which the supersaturation is reduced to zero. Indeed, the initial supersaturation for the dendrite in Figs. 3 and 2 is approximately the same; however, it is reduced to nearly zero for ~ 90 s (Fig. 3) in the first case and for ~ 160 s (Fig. 2) in the second case. Based on these time intervals, we have $b \approx 0.014$ and $b \approx 0.007$, respectively. If the supersaturation remained constant (as in the case of the examples considered in the Introduction), the supersaturation change would require an infinitely long time, and $b = 0$. Based on the above, it becomes clear that the factor b (as opposed to the factor a) is different for the different crystals observed in the experiments. Obviously, this factor also differs when the

same crystal is observed at different moments of time. Indeed, we can select sectors at different moments of time rather than one moment of time [as it was performed in Figs. 5(a) and 6(a)]. For example, we can place sector 0.1π on top of the primary branch 120 s before the crystal growth stops, allowing the behavior of $S'(t)/S(t)$ to be studied when the crystal grows through the sector (Fig. 10). This sector can also be placed on top of the primary branch (for example, 70 s before the crystal growth stops), and the measurements can be repeated. In the first case (120 s), $b \approx 0.007$, and in the second case (70 s), $b \approx 0.004$ (note that parameter a remains within the interval of 1.7 ± 0.2).¹¹

Thus, the brief analysis conducted herein shows that the factor a is of a sufficiently universal nature, and it is apparently connected with the growth regime.¹² It is known [19] that this regime is determined by the ratio between the rate of surface processes (this rate depends on the kinetic factor of crystallization and the characteristic size of the crystal) and the rate of the diffusion transfer in the solution (which is related to the diffusivity).¹³ The factor b is presumably not a universal characteristic of the crystallized system, and it evidently describes the unsteadiness inherent to spontaneous (uncontrolled) crystallization.

Let us nondimensionalize the obtained dependences $S(t)$ and $S'(t)/S(t)$. The time t^* of the crystal growth termination in the selected sector is the most important time for the problem under discussion. This time can be easily determined from the condition that $S'(t^*) = 0$. Clearly, $t^* = a/b$. Let us reduce the dependence of the area on time to the dimensionless form, so that $\tilde{S}(t^*) = 1$. Then, $\tilde{S}(\tilde{t}) = \tilde{t}^a \exp(a[1 - \tilde{t}])$ in dimensionless units, where the dimensionless time $\tilde{t} = t/t^*$, and the dimensionless area $\tilde{S} = S/[C(a/b)^a \exp(-a)]$. Thus,

¹¹In the second case, the supersaturation proves to be considerably lower than in the first case because the supersaturation decreases exponentially rather than linearly with time.

¹²For the fixed shape of the sector in which the observation is carried out and the fixed dimension of the problem.

¹³Essentially, the growth regime is determined by the basic physical and chemical parameters of the crystallized system [19].

TABLE II. Values of the two-parameter approximation $a/t - b$ of $S'(t)/S(t)$ for different sectors.

Factors \ Sectors	Sectors																
	a1	a2	a3	a4	a5	a6	a7	a8	a9	a10	s1	s2	s3	s4	s5	s6	s7
a	1.8	1.9	1.7	1.7	1.6	1.6	1.5	1.7	1.7	1.5	2.1	1.9	1.7	1.8	1.7	1.7	1.6
$b, \times 10^{-2}$	0.7	1.0	0.8	1.0	0.8	0.9	0.7	0.6	0.5	0.3	1.7	1.5	1.3	1.6	1.5	1.4	1.0

¹⁰It is clearly seen from the fact that $S(t) \sim \exp(-bt)$.

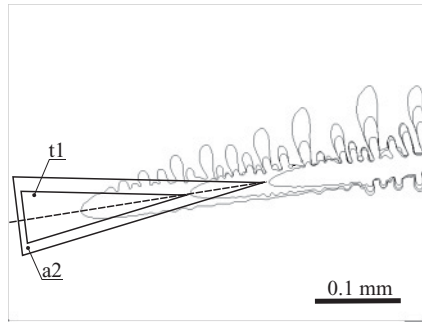


FIG. 10. Measurement of crystal area for two different intervals of dendrite growth time. Sector t1 allows the last 120 s of the dendrite growth to be measured, and sector a2 allows 160 s of the dendrite growth to be measured. This selection of sector t1 fundamentally differs from the case shown in Fig. 5 [in which all sectors allow $S(t)$ to be measured at the same time].

for dimensionless units, all time dependences of the crystal area obtained in the experiment are described with the one-parameter function $\tilde{t}^{1.7} \exp(1.7[1 - \tilde{t}])$ (Fig. 11).

If we use the same time scale, the normalized area increment has the form $\tilde{S}'/\tilde{S} = a(1/\tilde{t} - 1)$ or (based on the results of our experiments with the ammonium chloride crystallization) $\tilde{S}'/\tilde{S} = 1.7(1/\tilde{t} - 1)$. Figure 12 shows the extent to which the obtained and pre-non-dimensionalized data deviate from this universal dependence. For clarity, this graph is constructed using converted coordinates in which the dependence $\tilde{S}'/\tilde{S} = 1.7(1/\tilde{t} - 1)$ has the form of a linear function starting from the origin of the coordinate system. The presented results (Figs. 11 and 12) indicate that the obtained experimental data regarding the time dependence of the area and the normalized area increment can be described well (within 10%–15% error limits) using the simple one-parameter dependences after the corresponding normalization.

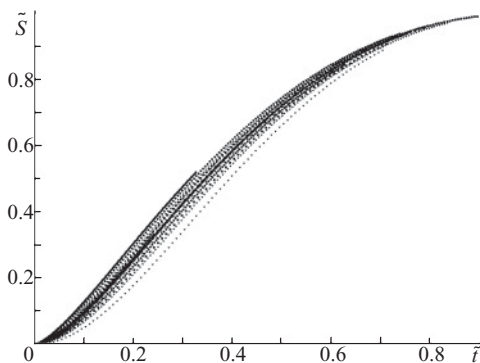


FIG. 11. Values of the nondimensionalized areas of all sectors shown in Figs. 5 and 6 relative to the nondimensionalized time. The nondimensionalization was carried out according to the rules given in the present paper. The parameters a and b for the nondimensionalization were individually taken from Table II for each sector.

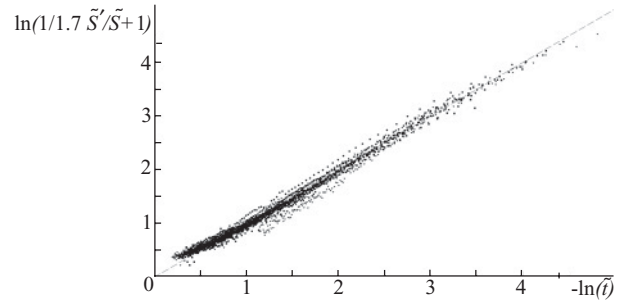


FIG. 12. Values of the nondimensionalized normalized area increment of all sectors shown in Figs. 5 and 6 relative to the nondimensionalized time. The nondimensionalization and conversion of the coordinate axes were carried out according to the rules given in the present paper. The parameters a and b for the nondimensionalization were individually taken from Table II for each sector.

IV. CONCLUSIONS

On the basis of the simplest geometrical reasoning, it is possible to advance a hypothesis of the universality of the normalized mass increment for a dendrite under unsteady growth.¹⁴ This hypothesis is confirmed in the present paper by the experiment with the quasi-two-dimensional crystallization of ammonium chloride from an aqueous solution. The dendrite area change divided by the area itself varies with time as $a/t - b$ for any sector oriented along the growth direction of the dendrite branches (primary or side). The values of the factors a and b are obtained, and their physical meaning is discussed. This result allows an analytical form of the curve to be proposed for description of the evolution of the dendrite area (or its part) with time; this analytical form can be expressed as follows: $S(t) = \text{const } t^a \exp(-bt)$.¹⁵ The nondimensionalization of quantities using the full dendrite growth time enables $S(t)$ and $S'(t)/S(t)$ to be reduced to simple one-parameter dependences, in which the parameter is presumably connected with the dendrite growth regime in the solution. The given results are the first to find a universal (invariant) characteristic for the primary and side dendrite branches under unsteady growth. Additional experiments with both ammonium chloride and other dendrite-forming substances are required for complete certainty of the obtained results and to provide further progress in the selected direction of the study.¹⁶

¹⁴Let us repeat here that universality is considered to be the equality of the normalized mass increments for different simultaneously growing dendrite branches.

¹⁵There is no definite opinion regarding this issue in the literature. In particular, the Weibull function is used to describe the dependence of the crystal mass (area) on time [17–19,30].

¹⁶Apparently, the obtained result for the area (in the case of the quasi-two-dimensional system) can be generalized to the crystal volume (for the three-dimensional case) and to the dendrite growth with arbitrary orientation with respect to cell borders. In that case, the values of the factors will certainly change.

- [1] J. Kepler, *Strena, Seu de Nive Sexangula, Francofurti ad Moenum* (1611), translated into English by C. Hardie, *The Six-Cornered Snowflake* (Clarendon Press, Oxford, 1966).
- [2] B. Chalmers, *Principles of Solidification* (Wiley, NY, 1964).
- [3] W. Kurz and D. J. Fisher, *Fundamentals of Solidification* (Trans. Tech. Pub., Aedermannsdorf, Switzerland, 1992).
- [4] D. M. Herlach, P. Galenko, and D. Holland-Moritz, *Metastable Solids from Undercooled Melts* (Elsevier, New York, 2007).
- [5] J. S. Langer, *Rev. Mod. Phys.* **52**, 1 (1980).
- [6] D. Kessler, J. Koplik, and H. Levine, *Adv. Phys.* **37**, 255 (1988).
- [7] E. A. Brener and V. I. Melnikov, *Adv. Phys.* **40**, 53 (1991).
- [8] M. E. Glicksman and S. P. Marsh, in *Handbook of Crystal Growth*, edited by D. T. J. Hurle (Elsevier, New York, 1993), Vol.1.
- [9] E. Ben-Jacob, *Contemp. Phys.* **34**, 247 (1993).
- [10] J. Feder, *Fractals* (Plenum, New York, 1988).
- [11] U. Bisang and J. H. Bilgram, *Phys. Rev. E* **54**, 5309 (1996).
- [12] M. B. Koss, J. C. Lacombe, L. A. Tennenhouse, M. E. Glicksman, and E. A. Winsa, *Metall. Mater. Trans. A* **30A**, 3179 (1999).
- [13] A. J. Melendez Ramirez, PhD dissertation, University of Iowa, 2009.
- [14] H. Ziegler, *An Introduction to Thermomechanics* (North-Holland, Amsterdam, 1983), p. 328.
- [15] *Non-Equilibrium Thermodynamics and the Production of Entropy in Life, Earth, and Beyond*, edited by A. Kleidon and R. D. Lorenz (Springer Verlag, Heidelberg, 2004), p. 382.
- [16] L. M. Martyushev and V. D. Seleznev, *Phys. Rep.* **426**, 1 (2006).
- [17] L. M. Martyushev, e-print [arXiv:1011.4137v1](https://arxiv.org/abs/1011.4137v1).
- [18] L. Mandelkern, *Crystallization of Polymers* (McGraw-Hill, New York, 1964).
- [19] A. A. Chernov, *Modern Crystallography III: Crystal Growth. Part I* (Springer, New York, 1984).
- [20] S.-K. Chan, H.-H. Reimer, and M. Kahlweit, *J. Cryst. Growth* **32**, 303 (1976).
- [21] H. Honjo, S. Ohta, and Y. Sawada, *Phys. Rev. Lett.* **55**, 841 (1985).
- [22] Y. Sawada, *Physica A* **140**, 134 (1986).
- [23] E. Raz, S. G. Lipson, and E. Polturak, *Phys. Rev. A* **40**, 1088 (1989).
- [24] H. Honjo and S. Ohta, *Phys. Rev. A* **45**, R8332 (1992).
- [25] L. Jun-Ming, L. Zhi-Guo, and W. Zhuang-Chun, *Scr. Metall. Mater.* **32**, 445 (1995).
- [26] E. G. Aksel'rod, L. M. Martyushev, and E. V. Levkina, *Tech. Phys. Lett.* **25**, 830 (1999).
- [27] A. Dougherty and M. Lahiri, *J. Cryst. Growth* **274**, 233 (2005).
- [28] A. Dougherty and T. Nunnally, *J. Cryst. Growth* **300**, 467 (2007).
- [29] R. C. Gonzalez, R. E. Woods, and S. L. Eddins, *Digital Image Processing using MATLAB* (Prentice Hall, Englewood Cliffs, NJ, 2004).
- [30] L. M. Martyushev and E. G. Axelrod, *J. Exp. Theor. Phys. Lett.* **78**, 476 (2003).